Inorg. Chem. **2006**, *45*, 4157−4166

Experimental and Theoretical Investigations of IR Spectra and Electronic Structures of the $U(OH)_2$, $UO_2(OH)$, and $UO_2(OH)_2$ Molecules

Xuefeng Wang and Lester Andrews*

Department of Chemistry, University of Virginia, McCormick Road, P.O. Box 400319, Charlottesville, Virginia 22904-4319

Jun Li*

William R. Wiley Environmental Molecular Sciences Laboratory, Pacific Northwest National Laboratory, Richland, Washington 99352

Received December 2, 2005

Reactions of laser-ablated U atoms and H_2O_2 molecules produce UO_2, H_2UO_2, and $UO_2(OH)_2$ as major products and $U(OH)_2$ and HU(O)OH as minor products. Complementary information is obtained from similar reactions of U atoms with D_2O_2, with $H_2 + O_2$ mixtures, and with H_2O in excess Ar. Through extensive relativistic density functional theory calculations, we have determined the geometry structures and ground states of these U species with a variety of oxidation states U^{II}, U^{IV}, U^{V}, and U^{VI}. The calculated vibrational frequencies, IR intensities, and isotopic frequency ratios are in good agreement with the experimental values, thus supporting assignments of the observed matrix IR spectra. We propose that the reactions proceed by forming an energized $[U(OH)_4]^*$ intermediate from reactions of the excited U atom with two H_2O_2 molecules. Because of the special stability of the U^{VI} oxidation state, this intermediate decomposes to the $UO_2(OH)_2$ molecule, which reveals a distinctive difference between the chemistries of U and Th, where the major product in analogous Th reactions is the tetrahedral $Th(OH)_4$ molecule owing to the stable Th^{IV} oxidation state.

Introduction

Although the ligated uranyl dication is involved extensively in U complexes, the bare UO_2^{2+} dication was not detected experimentally until 1996.[1] Because chemical properties of the free uranyl ion are still largely unknown, research on uranyl cations with simple ligands is therefore of great importance. Among the large number of uranyl complexes, uranyl dihydroxide, $UO_2(OH)_2$, has been a significant species for nuclear fuel production since the internal gelation process was developed in The Netherlands.[2] Researchers at the Oak Ridge National Laboratory and others have fully developed the internal gelation process for making UO_2, $UO_2 + PuO_2$, and $UO_2 + UC_2$ microspherical fuel elements. One of the four key reactions in the internal gelation process is the hydrolysis of UO_2^{2+} complexes where uranyl reacts with H_2O to form oxyhydrides in solution and x is the number of H_2O molecules that coordinate to the uranyl dication.

$$UO_2^{2+} + xH_2O = UO_2(OH)_2\cdot(x-2)H_2O + 2H^+$$

Through these processes, the soluble UO_2^{2+} complexes are transformed into a $UO_3\cdot 2H_2O$ or $UO_2(OH)_2\cdot H_2O$ gel, which is then reduced with H_2 and is calcined and sintered into a fuel kernel.[3] It has been proposed that the next generation of nuclear reactors will likely use coated microspherical UO_2 to improve safety and to increase the burning-up rate.

The monohydrate of solid uranium trioxide, UO_3, is actually uranyl dihydroxide, $UO_2(OH)_2$, which is an interesting compound in its own right. The structures of three

* To whom correspondence should be addressed. E-mail: lsa@virginia.edu (L.A.), jun.li@pnl.gov (J.L.).

(1) Cornehl, H. H.; Heinemann, C.; Marçalo, J.; Pires de Matos, A.; Schwarz, H. *Angew. Chem., Int. Ed. Engl*. **1996**, *35*, 891.

(2) van der Brugghens, F. W.; Noothout, A. J.; Hermans, M. E. A.; Kanij, J. B. W.; Votocek, O. A U(VI) Process for Microsphere Production. In *Proceedings of the Symposium on Sol−Gel Processes and Reactor Fuel Cycles*, Gatlinburg, TN, May 4−7, 1970; U.S. Atomic Energy Commission: Washington, DC, 1970; CONF-700502.

(3) Collins, J. L.; Hunt, R. D.; Del Cul, G. D.; Williams, D. F. *Production of Depleted UO_2 Kernels for the Advanced Gas-Cooled Reactor Program for Use in Triso Coating Development*; Oak Ridge National Laboratory: Oak Ridge, TN, Nov 2004; ORNL/TM-2004/123.

10.1021/ic052071a CCC: $33.50
Published on Web 04/20/2006

polymorphs of $UO_2(OH)_2$ have been determined.[4,5] The α form consists of octahedral $UO_2(OH)_4$ units, which make up a layer sharing all four equatorial OH groups, and is converted by slight pressure into the β form, where U has six OH neighbors in an equatorial plane approximately perpendicular to the UO_2 groups.[4] IR spectra of the solid $UO_2(OH)_2$ compounds reveal a sharp 3545-cm^{-1} band for O−H vibrations not modified by H bonding and broad O−H stretching bands near 3380 cm^{-1}, which are characteristic of OH groups involved in H bonding.[4] Solubility products and complex equilibria in the uranyl hydroxide system have also been investigated,[6] and such uranyl hydroxide species are involved in radioactive waste disposal processes.[7] In addition to the studies of uranyl hydroxides in the condensed phase, the gaseous $UO_2(OH)_2$ molecule is also an important species because it is expected to form from the reaction of nuclear fuel and H_2O in the case of a core meltdown.[8] Therefore, isolation of various uranyl hydroxides and the elucidation of their structures and bonding are key steps in understanding the chemical processes involved in nuclear fuel storage and nuclear waste processing.

In the theoretical aspect, there are recent computational studies on uranyl hydroxide complexes in the gas phase and uranyl hydrate species in solution, which are both important in nuclear waste disposal and nuclear fuel processing.[8−10] It is found that the $UO_2(OH)_2$ molecule has a slightly bent O═U═O angle as a result of π donation from the OH^- ligands to the UO_2^{2+} moiety,[8,9] and the structure is comparable to that found for UO_2F_2,[11,12] as confirmed in a recent theoretical investigation.[13] We also recently identified a uranyl dihydride molecule H_2UO_2 through reactions of laser-ablated U atoms with H_2O,[14] where the UO_2 unit is found to be bent in the gas phase but it seems to prefer a linear structure in the Ar matrix.

There appears to be no evidence for a pure uranium hydroxide $U(OH)_n$ solid material in the open literature, although activity products for $An(OH)_3$ (An = actinide) species have been tabulated,[15] and the crystal structure of $U(OH)_2SO_4$ has been determined.[16] Our previous experimental and theoretical investigations of U atoms reacting with H_2O molecules condensed in an Ar matrix have provided evidence for two more-stable structural isomers of $U(OH)_2$, namely, HU(O)OH and the aforementioned H_2UO_2.[14] We have subsequently developed a procedure for reacting laser-ablated transition-metal atoms with H_2O_2 to form metal dihydroxide molecules.[17−22] However, in the analogous reactions of Th with H_2O_2, the Th^{IV} complex $Th(OH)_4$ was the major product molecule and $Th(OH)_2$ and the HTh(O)OH isomer were minor products.[22] Because U has much richer oxidation states than Th, it is interesting to compare the chemistries of U and Th. We report here a combined experimental and theoretical study on the IR spectra of the Ar-matrix-isolated reaction products of laser-ablated U reacting with H_2O_2. Our results show that, unlike for Th, the stable U^{VI} complex $UO_2(OH)_2$ is formed as the major product because of the higher oxidation state of U. This is the first experimental identification of the isolated $UO_2(OH)_2$ molecule.

Experimental and Theoretical Methods

The techniques for co-deposited laser-ablated metal atoms with H_2O_2 have been described in earlier papers.[14,17−23] Briefly, urea/H_2O_2 (Aldrich) was placed in the side arm of a Chemglass stopcock and Ar was flowed over this volatile complex onto a CsI window at 10 K. U atoms from the ablation target were codeposited with this reagent stream. Deuterium-enriched material was prepared using methods reported earlier to exchange urea and H_2O_2 with D_2O.[24,25] Matrix IR spectra were recorded on a Nicolet 750 instrument after sample deposition, after annealing, and after irradiation using a Hg arc lamp (Sylvania, 175 W, globe removed). Experiments were also done with $H_2 + O_2$ mixtures to facilitate ^{18}O substitution.

We performed extensive calculations on the optimal geometries and the ground states of various U and uranyl hydroxide species using scalar relativistic density functional theory (DFT) methods. Several of these complexes studied are open-shell systems with potentially complicated multiplet structures from the $5f^n$ configuration.[26] Even though multireference ab initio electron correlation methods are, in principle, more appropriate in treating these complexes, these methods are computationally expensive and cannot be conveniently used to calculate the vibrational properties of these actinide molecules. Because of the low symmetry and the ligand

(4) Hoekstra, H. R.; Siegel, S. *J. Inorg. Nucl. Chem.* **1973**, *35*, 761 and references cited therein.
(5) Wells, A. F. *Structural Inorganic Chemistry*, 4th ed.; Clarendon Press: Oxford, U.K., 1975.
(6) Kramerschnabel, U.; Bischoff, H.; Xi, R. H.; Marx, G. *Radiochim. Acta* **1992**, *56*, 183.
(7) Clark, D. L.; Conradson, R. J.; Donohoe, R. J.; Keogh, D. W.; Morris, D. E.; Palmer, P. D.; Rogers, R. D.; Tait, C. D. *Inorg. Chem.* **1999**, *38*, 1456.
(8) (a) Schimmelpfenning, B.; Privalov, T.; Wahlgren, U.; Grenthe, I. *J. Phys. Chem. A* **2003**, *107*, 9705 and references cited therein. (b) Shamov, G. A.; Schreckenbach, G. *J. Phys. Chem. A* **2005**, *109*, 10961. (c) Sonnenberg, J. L.; Hay, P. J.; Martin, R. L.; Bursten, B. E. *Inorg. Chem.* **2005**, *44*, 2255.
(9) Oda, Y.; Aoshima, A. *J. Nucl. Sci. Technol.* **2002**, *39*, 647.
(10) Tsushime, S.; Reich, T. *Chem. Phys. Lett.* **2001**, *347*, 127.
(11) Wang, Q.; Pitzer, R. M. *J. Phys. Chem. A* **2001**, *105*, 8370.
(12) (a) Straka, M.; Dyall, K. G.; Pyykko, P. *Theor. Chem. Acc.* **2001**, *106*, 393. (b) Kovacs, A.; Konings, R. J. M. *J. Mol. Struct. (THEOCHEM)* **2004**, *684*, 35.
(13) Hratchen, H. P.; Sonnenberg, J. L.; Hay, P. J.; Martin, R. L.; Bursten, B. E.; Schlagel, H. B. *J. Phys. Chem. A* **2005**, *109*, 8579.
(14) Liang, B.; Hunt, R. D.; Kushto, G. P.; Andrews, L.; Li, J.; Bursten, B. E. *Inorg. Chem.* **2005**, *44*, 2159.
(15) Katz, J. J., Seaborg, G. T., Morss, L. R., Eds. *The Chemistry of the Actinide Elements*, 2nd ed.; Chapman and Hall: London, 1986; pp 1288−1290.
(16) Lundgren, G. *Ark. Kemi* **1952**, *4*, 421.
(17) (a) Andrews, L.; Wang, X. *Inorg. Chem.* **2005**, *44*, 11. (b) Wang, X.; Andrews, L. *J. Phys. Chem. A* **2005**, *109*, 2782.
(18) Wang, X.; Andrews, L. *J. Phys. Chem. A* **2005**, *109*, 3849.
(19) (a) Wang, X.; Andrews, L. *Chem. Commun.* **2005**, 4001. (b) Wang, X.; Andrews, L. *Inorg. Chem.* **2005**, *44*, 9076.
(20) (a) Wang, X.; Andrews, L. *Inorg. Chem.* **2005**, *44*, 7189 (Hf + H_2O_2). (b) Wang, X.; Andrews, L. *J. Phys. Chem. A* **2005**, *109*, 10689 (group 4).
(21) Wang, X.; Andrews, L. *J. Phys. Chem. A* **2005**, *109*, 9013 (Pb + H_2O_2).
(22) Wang, X.; Andrews, L. *Phys. Chem. Chem. Phys.* **2005**, *7*, 3834 (Th + H_2O_2).
(23) Andrews, L. *Chem. Soc. Rev.* **2004**, *33*, 123 and references cited therein.
(24) Pettersson, M.; Tuominen, S.; Rasanen, M. *J. Phys. Chem. A* **1997**, *101*, 1166.
(25) Pehkonen, S.; Pettersson, M.; Lundell, J.; Khriachtchev, L.; Rasanen, M. *J. Phys. Chem. A* **1998**, *102*, 7643.
(26) Clavaguera-Sarrio, C.; Vallet, V.; Maynau, D. Marsden, C. J. *J. Chem. Phys.* **2004**, *121*, 5312.

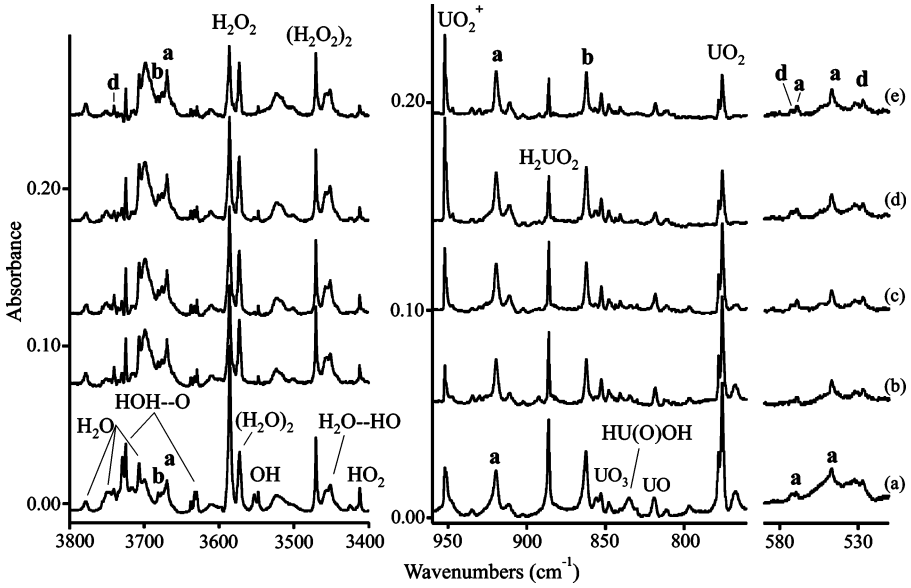

Figure 1. IR spectra in the 3800−3400-, 960−760-, and 590−510-cm^{-1} regions for the products of laser-ablated U atom reactions with H_2O_2 molecules in excess Ar at 12 K: (a) after sample deposition for 60 min, (b) after annealing to 26 K, (c) after irradiation at 240−380 nm for 20 min, (d) after irradiation at >220 nm for 20 min, and (e) after annealing to 32 K.

field splitting of the open-shell systems studied here, the multiplet problems of these U complexes are much simpler, and DFT methods can provide a reasonably accurate description of the ground-state geometries and vibrational frequencies. We choose to use both the generalized gradients approximation (GGA) and hybrid GGA methods to validate the accuracy of the DFT methods for these low-valent U complexes and to provide a comparison within the theoretical approach. Spin−orbit coupling effects usually do not have significant effects for the ground-state geometries and vibrational frequencies and were not included in the calculations. The structures and vibrational frequencies of potential product molecules were calculated using both ADF and NWChem program systems.[27,28] The ADF calculations used the relativistic zero-order regular approximation (ZORA)[29] and the PW91 functional with TZ2P basis sets,[30] and the computational details are the same as those used for the U/H_2O reaction products.[14] In the NWChem calculations, we used the popular B3LYP hybrid exchange-correlation functional in the DFT calculations.[31−33] The Stuttgart relativistic small-core (60-electron) pseudopotential was used for U, and corresponding U [8s7p6d4f] valence basis sets were augmented by two g-type polarization functions (1.2649 and 0.5060).[34,35] For O and H, we used all-electron aug-cc-pVTZ basis sets developed by Dunning and co-workers.[36,37] An extra-fine integration grid and a stringent convergence criterion were used in geometry optimizations.

Results

Reactions of energetic U atoms and H_2O_2 molecules formed a series of small U-containing molecules. We will examine the IR spectra of several new actinide hydroxide molecules, which are identified by isotopic frequency shifts and comparison of the calculated vibrational frequencies and IR intensities with experiments.

IR Spectra. Four experiments were done with laser-ablated U atoms and H_2O_2 molecules using different laser energies and reagent concentrations, and IR spectra from the highest product yield experiment are illustrated in Figure 1. The upper region shows the strong 3587-cm^{-1} H_2O_2 monomer absorption and weaker 3470- and 3458-cm^{-1} dimer and multimer bands[17−22,24] and product features at 3730, 3725.3, 3633, and 3630.1 cm^{-1} for the HOH- -O complex,[18,25] at 3778, 3755, 3707, 3702, 3638, and 3574 cm^{-1} for H_2O species,[38] at 3553.0 and 3548.0 cm^{-1} for the OH radical,[39] a shoulder at 3452 cm^{-1} for the H_2O/HO complex,[40,41] and 3412.3 cm^{-1} for the HO_2 radical,[42,43] which are common to

(27) ADF 2004.01, SCM, Theoretical Chemistry, Vrije Universiteit, Amsterdam, The Netherlands (www.scm.com).
(28) Aprà, E.; Windus, T. L.; Straatsma, T. P.; Bylaska, E. J.; de Jong, W.; Hirata, S.; Valiev, M.; Hackler, M.; Pollack, L.; Kowalski, K.; Harrison, R.; Dupuis, M.; Smith, D. M. A.; Nieplocha, J.; Tipparaju V.; Krishnan, M.; Auer, A. A.; Brown, E.; Cisneros, G.; Fann, G.; Früchtl, H.; Garza, J.; Hirao, K.; Kendall, R.; Nichols, J.; Tsemekhman, K.; Wolinski, K.; Anchell, J.; Bernholdt, D.; Borowski, P.; Clark, T.; Clerc, D.; Dachsel, H.; Deegan, M.; Dyall, K.; Elwood, D.; Glendening, E.; Gutowski, M.; Hess, A.; Jaffe, J.; Johnson, B.; Ju, J.; Kobayashi, R.; Kutteh, R.; Lin, Z.; Littlefield, R.; Long, X.; Meng, B.; Nakajima, T.; Niu, S.; Rosing, M.; Sandrone, G.; Stave, M.; Taylor, H.; Thomas, G.; van Lenthe, J.; Wong, A.; Zhang, Z. *NWChem, A Computational Chemistry Package for Parallel Computers*, version 4.6; Pacific Northwest National Laboratory: Richland, WA, 2004.
(29) van Lenthe, E.; Baerends, E. J.; Snijders, J. G. *J. Chem. Phys*. **1993**, *99*, 4597.
(30) (a) Perdew, J. P.; Wang, Y. *Phys. Rev. B* **1992**, *45*, 13244. (b) van Lenthe, E.; Baerends, E. J. *J. Comput. Chem.* **2003**, *24*, 1142.
(31) Becke, A. D. *J. Chem. Phys*. **1993**, *98*, 1372.
(32) Lee, C.; Yang, W.; Parr, R. G. *Phys. Rev. B* **1988**, *37*, 785.
(33) Stephens, P. J.; Devlin, F. J.; Chabalowski, C. F.; Frisch, M. J. *J. Phys. Chem*. **1994**, *98*, 11623.
(34) Küchle, W.; Dolg, M.; Stoll, H.; Preuss, H. *J. Chem. Phys.* **1994**, *100*, 7535.
(35) Ismail, N.; Heully, J.-L.; Saue, T.; Daudey, J.-P.; Marsden, C. J. *Chem. Phys. Lett.* **1999**, *300*, 296.
(36) Dunning, T. H., Jr. *J. Chem. Phys*. **1989**, *90*, 1007.
(37) Kendall, R. A.; Dunning, T. H., Jr.; Harrison, R. J. *J. Chem. Phys*. **1992**, *96*, 6796.
(38) Ayers, G. P.; Pullin, A. D. E. *Spectrochim. Acta* **1976**, *32A*, 1629.
(39) Cheng, B.-M.; Lee, Y.-P.; Ogilvie, J. F. *Chem. Phys. Lett.* **1988**, *109*, 151.
(40) Langford, V. S.; McKinley, A. J.; Quickenden, T. I. *J. Am. Chem. Soc.* **2000**, *122*, 12859.
(41) Cooper, P. D.; Kjaergaard, H. G.; Langford, V. S.; McKinley, A. J.; Quickenden, T. I.; Schofield, D. P. *J. Am. Chem. Soc.* **2003**, *125*, 6048.
(42) Milligan, D. E.; Jacox, M. E. *J. Chem. Phys.* **1963**, *38*, 2627.
(43) Smith, D. W.; Andrews, L. *J. Chem. Phys.* **1974**, *60*, 81.

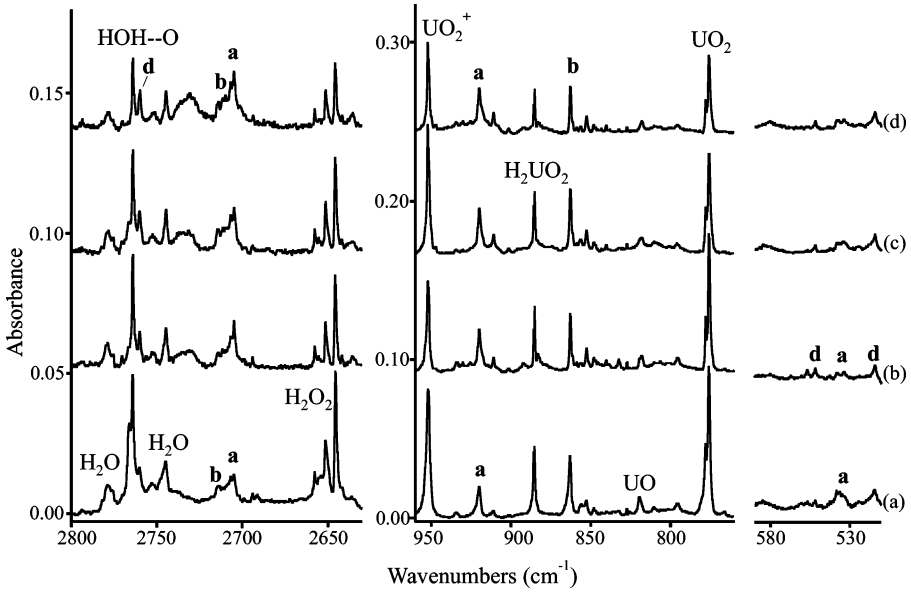

Figure 2. IR spectra in the 2800−2630-, 960−760-, and 590−510-cm^{-1} regions for the products of laser-ablated U atom reactions with D_2O_2 molecules in excess Ar at 12 K: (a) after sample deposition for 60 min, (b) after annealing to 26 K, (c) after irradiation at >220 nm for 20 min, and (d) after annealing to 32 K.

H_2O_2 experiments with laser-ablated metal atoms.[17−22] New U product absorptions are observed at 3740.6 cm^{-1} (labeled **d**) and at 3681.6 and 3669.9 cm^{-1} (labeled **b** and **a**, respectively). The lower region contains strong bands due to UO_2^+ at 952.3 cm^{-1} and UO_2 at 775.6 cm^{-1} and weaker bands due to UO and UO_3 that have been observed previously.[44−47] The sharp 886.0-cm^{-1} product absorption and associated 1406-cm^{-1} feature have recently been identified in the U and H_2O matrix system as H_2UO_2, and weak 1370-, 834-, and 576-cm^{-1} bands were observed for the HU(O)OH isomer.[14] Two new absorptions at 919.6 and 862.2 cm^{-1} (labeled **a** and **b**, respectively) are the subject of the present investigation. New weak bands were also observed at 569.0, 546.8, and 526.6 cm^{-1} (labeled **a**, **a**, and **d**, respectively). The samples were subjected to a sequence of annealing cycles and UV irradiations, and both UO_2^+ and UO_2 bands decreased upon annealing. However, the cation increased and the molecule decreased upon UV irradiation, while the **d** absorption slightly decreased and the other product absorptions slightly increased.

Two experiments were performed with deuterium-enriched D_2O_2 samples, and IR spectra from the three regions are shown in Figure 2. The spectra are dominated by D_2O_2 at 2645 cm^{-1} and by a DOD- -O complex at 2764.1 cm^{-1}, and D_2O bands appear at 2778 and 2745 cm^{-1}. Bands for OD were observed lower at 2615.7 and 2613.9 cm^{-1}, for the D_2O_2 dimer at 2564 cm^{-1}, and for D_2O/DO at 2542.7 cm^{-1}.[18,24,25] The new product absorptions were observed at 2760.0 cm^{-1} (labeled **d**) and at 2714.0 and 2704.8 cm^{-1} (labeled **b** and **a**, repectively). The middle region appears to the eye, as shown in Figure 1, but the new product absorptions shift slightly to 919.9, 885.2, and 862.7 cm^{-1}. In the low region, weak new bands are observed at 551.8, 538.1, and 514.1 cm^{-1} (labeled **d**, **a**, and **d**, respectively).

The U atom reaction with higher-concentration $H_2 + O_2$ mixtures gave the IR spectra in Figure 3. The upper region shows stronger H_2O absorptions, a weaker HOH- -O complex at 3725.6 and 3630.1 cm^{-1}, a weak H_2O_2 band at 3586.1 cm^{-1}, and almost the same **a** and **b** bands at 3682.4 and 3670.0 cm^{-1}, which reach about one-third of their intensity with the H_2O_2 reagent. The **d** band was not present at 3740.7 cm^{-1}. Interestingly, the H_2O/HO band at 3452.3 cm^{-1} appeared and the H_2O dimer band at 3574 cm^{-1} increased upon UV irradiation, but the isolated OH radical was not observed. The lower region exhibits a stronger uranium oxide species and the same but weaker product absorptions, which are listed in Table 1. The new product absorptions increase at a higher proportion upon UV irradiation, particularly the **a** band pair. In addition, weak uranium hydride bands were observed.[48] Similar experiments were done with D_2 and with $^{18}O_2$, and the shifted product absorptions are also given in Table 1. A weak **d** band was detected at 2760.0 cm^{-1}.

Experiments were further performed with $H_2 + O_2$ isotopic mixtures, and the IR spectra are compared in Figure 4 with spectra for the $^{16}O_2$ and $^{18}O_2$ reaction products. The original-deposited-sample spectrum and the spectrum recorded after the UV irradiation, annealing to 18−20 K, and a second UV irradiation sequence are shown for each sample. The $^{16}O_2 + {}^{18}O_2$ mixture reveals isotopic doublets for each major product absorption (Figure 4b), but the $^{16}O_2 + {}^{16}O^{18}O + {}^{18}O_2$ mixture provides the same doublet for the strong upper band and an isotopic triplet absorption pattern for each lower band (Figure 4c). (Unfortunately, the ^{18}O **b** band is masked by the ^{16}O **a** band.)

(44) Gabelnick, S. D.; Reedy, G. T.; Chasanov, M. G. *J. Chem. Phys.* **1973**, *58*, 4468; **1973**, *59*, 3697.
(45) Hunt, R. D.; Andrews, L. *J. Chem. Phys.* **1993**, *98*, 3690.
(46) Zhou, M.; Andrews, L.; Ismail, N.; Marsden, C. *J. Phys. Chem. A* **2000**, *104*, 5495.
(47) Wang, X.; Andrews, L.; Li, J.; Bursten, B. E. *Angew. Chem., Int. Ed.* **2004**, *43*, 2554.
(48) Souter, P. F.; Kushto, G. P.; Andrews, L.; Neurock, M. *J. Am. Chem. Soc.* **1997**, *119*, 1682.

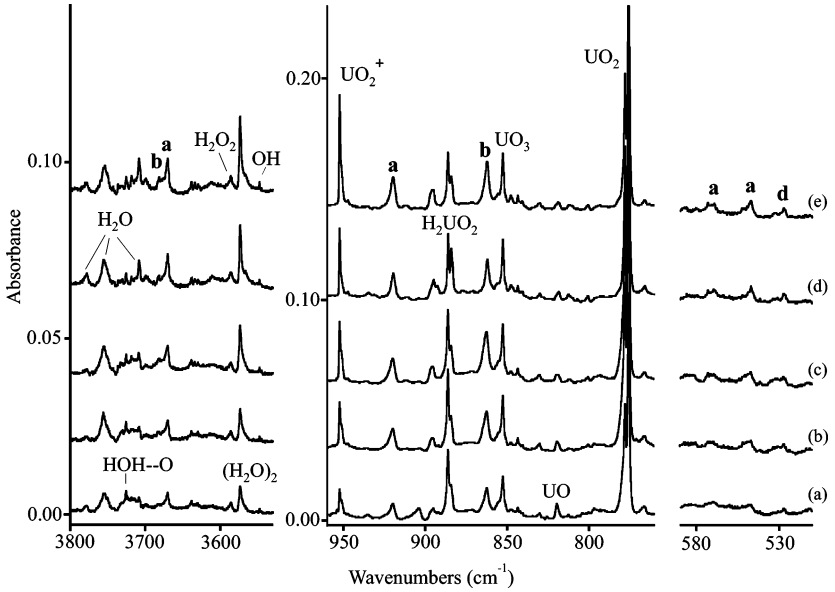

Figure 3. IR spectra in the 3800−3400-, 960−760-, and 590−510-cm^{-1} regions for the products of laser-ablated U atom reactions with H_2 (6%) and O_2 (0.4%) in excess Ar at 12 K: (a) after sample deposition for 60 min, (b) after irradiation at 240−380 nm for 20 min, (c) after irradiation at >220 nm for 20 min, (d) after annealing to 18 K, and (e) after irradiation at >220 nm for 20 min.

Table 1. IR Absorptions (cm^{-1}) Produced by Reactions of Laser-Ablated U Atoms and $H_2 + O_2$ Mixtures

$H_2 + {}^{16}O_2$	$H_2 + {}^{18}O_2$	$^{16}O/^{18}O$ ratio	$D_2 + {}^{16}O_2$	$D_2 + {}^{18}O_2$	identification
3725.4	3711.4	1.00377	2764.4	2750.4	HOH···O
3682.4	3670.7	1.00319	2714.7	2697.9	b, $UO_2(OH)$
3670.0	3658.8	1.00306	2704.9	2688.7	a, $UO_2(OH)_2$
3573.7	3565.1	1.00241	2614.0	2602.0	$(H_2O)_2$
3452.3	3441.3	1.00320	2543.1	2527.6	H_2O/HO
3412.3	3399.8	1.00368	2529.7	2514.1	HO_2
952.3	904.7	1.05261	952.3	904.7	UO_2^+
919.7	874.0	1.05229	920.3	874.6	a, $UO_2(OH)_2$
886.6	842.2	1.05252	885.3	841.2	H_2UO_2
862.2	819.5	1.05210	862.9	819.9	b, $UO_2(OH)$
852.5	810.0	1.05272	852.5	810.0	UO_3
819.8	775.5	1.05712	819.7	(775.8)	UO
745.6	705.1	1.05714	745.6	705.1	UO_3
569.2	552.0				a, $UO_2(OH)_2$
547.2	523.8		534		a, $UO_2(OH)_2$
527.5	503.5				b, $UO_2(OH)$

New experiments were done with CCl_4 added to the sample to serve as an electron trap and thereby favor the yield of cation products with each reaction system.[49] In each case, the UO_2^+ absorption intensity was increased relative to that for UO_2, but the relative yield of the **a** and **b** bands was not changed. Hence, we must conclude that the reaction products are neutral species.

Finally, the previous U/H_2O Ar matrix spectra[14] were examined for the present new product absorptions. Figure 5 illustrates spectra in the 3800−3650-cm^{-1} region from the experiment shown for the lower region in Figure 1 of ref 14. Weak **a** bands were observed at 3670.0 and 919.6 cm^{-1} (absorbance $A = 0.007$), which sharpened on the annealing cycles; however, the **b** bands were not observed in the H_2O experiments. A sharp, weak 3740.7-cm^{-1} absorption (labeled **d**) observed upon sample deposition increased stepwise (to $A = 0.08$) upon annealing and tracked with the unknown X band[14] at 570.5 cm^{-1} and another band at 527.3 cm^{-1} (not shown). Another sharp band at 3730.0 cm^{-1} increased on early annealing cycles and then decreased upon final annealing in step with the lower HU(O)OH bands. In the best ^{18}O-enriched H_2O experiment (90% ^{18}O in the deposited sample), these bands shifted to 3729.3, 3718.2, and 3658.8 cm^{-1}. In the D_2O experiments, 2760.0-, 551.8-, and 514.3-cm^{-1} species **d** bands behaved similarly and reached absorbances of 0.04, 0.015, and 0.02, respectively, upon annealing to 34 K. A mixed H_2O/HOD/D_2O (about equal H and D) experiment revealed both H and D counterpart species **d** bands, with the D doubling the absorbance on the H counterparts. Both H_2UO_2 and D_2UO_2 and also HU(O)OH and DU(O)OD products were observed with comparable intensities. Table 2 collects the isotopic absorptions for the new product absorption favored in H_2O experiments.

Calculations. Geometry structures and vibrational frequencies were calculated for several anticipated products of the reaction system. Inasmuch as the vibrational properties provide a sensitive probe for the ground-state geometries and electronic structures, we performed extensive searches of the minimum structures. For $UO_2(OH)_2$, structures with linear and bent U−O−H angles and with linear and bent uranyl units are all considered. Some selected structures that have been searched and optimized are shown in Figure 6. It turns out that the structure with a bent uranyl unit (Figure 6c) is much higher in energy than any linear or pseudolinear uranyl structures, consistent with the well-known fact that uranyl strongly prefers to be linear. Among the structures with linear or pseudolinear uranyl units, the two lowest-energy structures with C_2 (trans) and C_s (cis) symmetry (parts d and e of Figure 6, respectively) are nearly degenerate in energy. They are the lowest minimum energy structures but can hardly be differentiated at the DFT level of theory; the C_s structure is only 0.03 and 0.12 kcal/mol lower in energy than the C_2 structure from NWChem B3LYP and ADF PW91 calcula-

(49) Andrews, L.; Citra, A. *Chem. Rev.* **2002**, *102*, 885 and references cited therein.

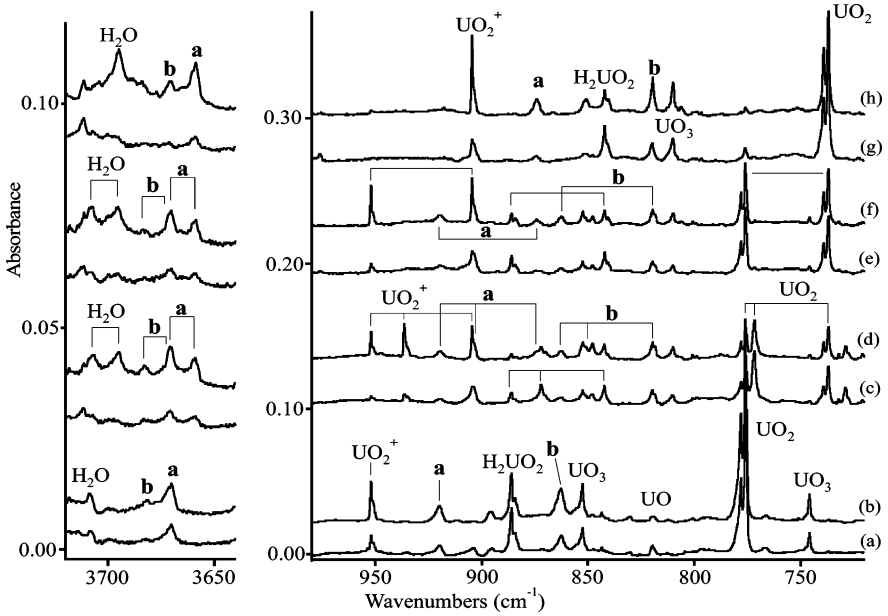

Figure 4. IR spectra in the 3720−3640- and 980−720-cm^{-1} regions for the products of laser-ablated U atom reactions with H_2 (6%) and isotopic O_2 samples in excess Ar at 12 K: (a) after sample deposition for 60 min with $^{16}O_2$ (0.4%), (b) after irradiation at >220 nm for 20 min, annealing to 18 K, and more irradiation at >220 nm for 20 min, (c) spectrum after deposition with scrambled $^{16}O_2$, $^{16}O^{18}O$, and $^{18}O_2$ (2/5/3) (0.5% total), (d) after the same treatment as that in part b, (e) after deposition with mixed $^{16}O_2$ and $^{18}O_2$ (0.4% each), (f) after that same treatment as that in part b, (g) after deposition with $^{18}O_2$ (0.6%), and (h) after the same treatment as that in part b.

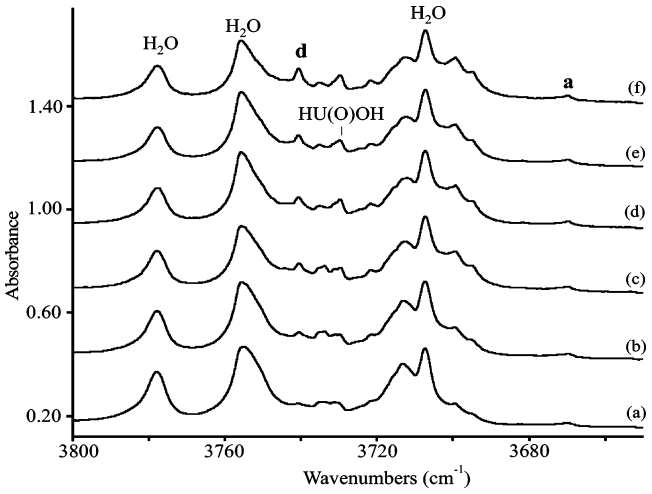

Figure 5. IR spectra in the 3800−3650-cm^{-1} region for laser-ablated U atoms codeposited with 0.2% H_2O in Ar at 7 K: (a) after sample deposition for 70 min, (b) after annealing to 25 K, (c) after annealing to 30 K, (d) after irradiation at >290 nm, (e) after irradiation at >220 nm, and (f) after annealing to 35 K.

Table 2. IR Absorptions (cm^{-1}) Observed for the **d** Product Favored in U and H_2O Reactions

H_2O	H_2O_2	$H_2{}^{18}O$	D_2O	D_2O_2
3740.7	3740.7	3729.3	2760.0	2760.0
570.5	571 sh		551.8	551.8
527.0	526.7		514.3	514.1

tions, respectively. From single-point CCSD(T) calculations based on the B3LYP geometries, the trans structure is 0.46 kcal/mol more stable than the cis structure. Because the calculated bond lengths, energetics, and vibrational properties of these two structures are similar, we will only discuss those of the trans structure.

Through a similar geometry search, we determined the lowest-energy structures of other species, and the structures

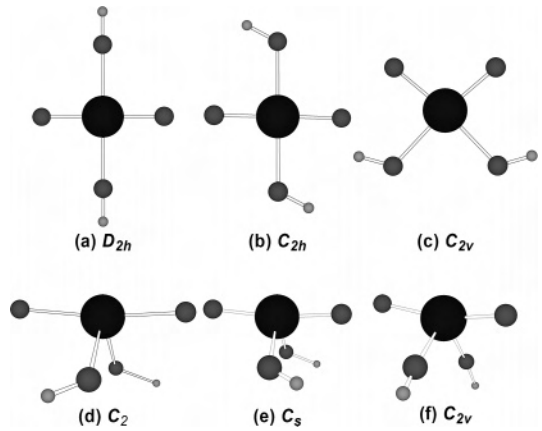

Figure 6. Six optimized structures for $UO_2(OH)_2$: (a) D_{2h} (10.2 kcal/mol, $N_{Imag} = 3$), (b) C_{2h} (2.3 kcal/mol, $N_{Imag} = 1$), (c) C_{2v} (11.8 kcal/mol, $N_{Imag} = 0$), (d) C_2 (0.1 kcal/mol, $N_{Imag} = 0$), (e) C_s (0.0 kcal/mol, $N_{Imag} = 0$), and (f) C_{2v} (4.8 kcal/mol, $N_{Imag} = 2$). The relative energies are from ZORA PW91/TZ2P calculations.

of $U(OH)_2$, $U(OH)_4$, $UO_2(OH)_2$ (C_2), and $UO_2(OH)$ are illustrated in Figure 7. Only one of these molecules, $UO_2(OH)_2$, has been calculated previously, and the results give bond lengths and angles very similar to those calculated and comparable frequencies.[8,9,13,50] From our calculations, the trans C_2 structure has U═O, U−OH, and O−H bond lengths of 1.805, 2.117, and 0.971 Å, respectively, with the O═U═O angle of 171.8° and the HO−U−OH bond angle of 108.4°. As shown in Figure 6, a C_{2v} structure (Figure 6f) with two imaginary frequencies ($N_{Imag} = 2$) is about 5 kcal/mol higher in energy, and following the imaginary modes, we located the trans and cis structures mentioned above. In addition, the D_{2h} structure with $N_{Imag} = 3$ is 10 kcal/mol

(50) Privalov, T.; Schimmelpfennig, B.; Wahlgren, U.; Grenthe, I. *J. Phys. Chem. A* **2002**, *106*, 11277.

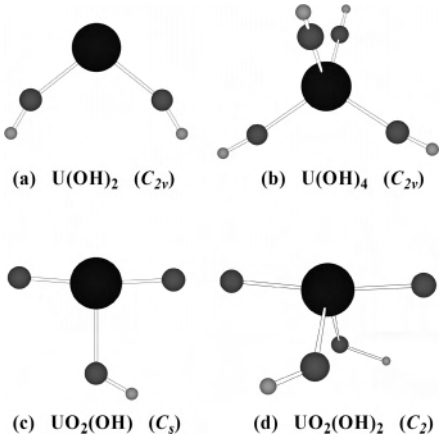

Figure 7. Structures calculated for U(OH)$_2$, U(OH)$_4$, UO$_2$(OH)$_2$, and UO$_2$-(OH) at the PW91 level of theory.

higher than the minimum energy structure, and two C_{2h} structures with in-plane and out-of-plane O−H bending have higher energies and imaginary frequencies.

Theoretical calculations show that UO$_2$(OH) is a U f^1 complex with C_s symmetry (Figure 7c), similar to the T-shaped structure of UO$_3$. This structure can be derived by removal of an OH group from the trans or cis structures of UO$_2$(OH)$_2$. The geometry parameters are very similar to those of UO$_2$(OH)$_2$, as expected.

The U(OH)$_2$ molecule is an interesting and rare U^{II} complex, which is found to have a stable C_{2v} structure (Figure 7a) with a U (7s)^1(5f)^3 configuration and a ^{5}A$_2$ ground state when spin−orbit coupling is not considered. Vibrational frequency calculations indicate that this structure is a real minimum on the potential energy surface. The U−OH distance is optimized to be 2.07 Å, and the O−U−O and U−O−H angles are 102.8° and 159.0°, respectively. The significantly bent O−U−O and U−O−H angles indicate that the attachment of H atoms to the oxo groups of UO$_2$ has greatly reduced the U≡O triple bonding. However, the U−O bond seems to still involve partial multiple-bond character because of the short U−O distance, which is even shorter than that in other high-valent U complexes. This U(OH)$_2$ molecule is a structural isomer of two more-stable structures that were reported in our previous work:[14] the HU(O)OH isomer is 24 kcal/mol more stable and the H$_2$UO$_2$ isomer is 36 kcal/mol more stable than the dihydroxide based on the present ADF calculations.

The geometry optimization of the U(OH)$_4$ molecule started with T_d symmetry, but the calculations converge to a $(a_1)^1$-$(t_2)^1$ electron configuration, which is subject to the first-order Jahn−Teller distortion expected for a U^{IV} complex. Subsequent geometry optimizations using D_{2d} and its C_{2h}, C_i, and C_s subgroups lead to structures with lower energies, but these structures are not minima. Following the imaginary modes of the T_d symmetry, we located the lowest-energy structure with C_{2v} symmetry (Figure 7b), which is very close to tetrahedral symmetry except that that the U−O−H angles are slightly bent (177.5° and 173.4°). Geometry optimizations using C_2 symmetry converge back to this C_{2v} structure, indicating that no further energy can be gained by lowering the symmetry. In the C_{2v} structure, the four OH groups are divided into two sets, with U−OH distances of 2.08 and 2.10 Å and O−U−O bond angles of 113.1° and 106.8°, respectively.

The calculated vibrational frequencies are compared for these uranium hydroxide species in Table 3 using both the PW91 and B3LYP density functionals implemented in ADF and NWChem programs. As is expected, the frequencies are generally calculated slightly higher with B3LYP than with PW91 because of the mixing of the Hartree−Fock exchange in the B3LYP method. The antisymmetric stretching mode of H$_2$O was calculated at 3808 cm^{-1} (PW91) and 3899 cm^{-1} (B3LYP), respectively, which provides a useful calibration mark for comparison to the experimental frequency of the gas-phase H$_2$O molecule at 3756 cm^{-1}.[51]

Discussion

The new product absorptions will be identified through the effect of isotopic substitution and comparison to frequencies calculated for anticipated products using DFT.

UO$_2$(OH)$_2$ and UO$_2$(OH). The **a** and **b** product absorptions were stronger and sharper in the H$_2$O$_2$ reactions than with the H$_2$ + O$_2$ reagent, but the product frequencies were nearly the same. The H/D isotopic frequency ratios, 1.3565 and 1.3568, and the ^{16}O/^{18}O isotopic frequency ratios, 1.00319 and 1.00306, for the upper 3682.4- and 3670.0-cm^{-1} **b** and **a** bands are characteristic of O−H(D) stretching modes.[17−22] The ^{16}O/^{18}O isotopic frequency ratios of the 919.7- and 862.2-cm^{-1} absorptions, 1.05229 and 1.05210, are characteristic of antisymmetric O═U═O stretching modes of a linear moiety.[44−46] In contrast, the U═O diatomic ^{16}O/^{18}O isotopic frequency ratio is 1.05712 (Table 1). The former bands exhibit small blue deuterium shifts, which may be more a consequence of line sharpening than a mechanical effect. Furthermore, the 919.7- and 862.2-cm^{-1} absorptions are in the region between the 952.3- and 775.7-cm^{-1} antisymmetric O═U═O stretching modes for UO$_2^+$ and UO$_2$, and related molecules must be considered. These latter bands exhibit no deuterium shifts.

The doublet patterns for the 919.7- and 862.2-cm^{-1} bands using the ^{16}O$_2$ + ^{18}O$_2$ mixture show that a single dioxygen molecule is incorporated into these products, and the triplet patterns with the ^{16}O$_2$ + ^{16}O^{18}O + ^{18}O$_2$ mixture demonstrate that two equivalent O atoms are involved in these vibrational motions. Hence, we are dealing with two new products that contain the O═U═O moiety and O−H substituents. There is not sufficient coupling between the O−H groups to cause any isotopic shift when ^{16}O$_2$ + ^{16}O^{18}O + ^{18}O$_2$ is employed so we conclude that two O−H groups are involved in the major **a** product because of the higher yield using the H$_2$O$_2$ reagent and that a single O−H group is likely involved in the **b** product, which is stronger using the H$_2$ + O$_2$ reagent.

The calculated frequencies in Table 3 define a pattern that fits the observed frequencies. The lowest O−H stretching

(51) Herzberg, G. *Infrared and Raman Spectra of Polyatomic Molecules*; D. van Nostrand: Princeton, NJ, 1945; p 281.

Table 3. Unscaled Vibrational Frequencies (cm^{-1}) and IR Absorption Intensities (km/mol) Calculated for Anticipated Products of the U and H_2O_2 Reaction Using PW91 (ADF) and B3LYP (NWChem) Methods[a]

$U(OH)_2$			$U(OH)_4$			$UO_2(OH)_2$			$UO_2(OH)$		
PW91	B3LYP	Int.	PW91	B3LYP	Int.	PW91	B3LYP	Int.	PW91	B3LYP	Int.
3787	3904	151	3787	3894	1	3731	3845	43	3737	3861	73
3786	3902	134	3787	3880	153	3727	3844	164	880	894	526
600	589	75	3771	3879	127	916	944	448	820	848	9
534	549	160	3770	3877	120	840	878	13	540	549	108
394	365	49	607	628,	4	562	572	87	511	531	100
312	327	163	581	572	298	545	556	49	504	449	145
261	233	170	564	569	311	518	544	34	194	211	17
220	212	0	562	568	285	514	534	413	178	187	25
101	114	0	372	399	139	468	488	162	126	134	41
			359	396	0	446	476	7			
			353	392	126	204	232	7			

[a] IR intensities (Int.) are in km/mol, calculated by NWChem.

frequency for a neutral species correlates with the higher O═U═O stretching frequency, and the **a** bands are assigned to the $UO_2(OH)_2$ molecule. In the corresponding $UO_2(OH)^+$ cation, the O−H stretching frequency is too low and the O═U═O frequency is too high relative to the a bands to fit the **b** absorptions, and recall that the cation identification has been ruled out by the electron-trap doping experiment. Because of the approximate treatments of electron correlation in the DFT methods and the use of the harmonic approximation in frequency calculations, scaling factors are usually needed to compare frequencies from harmonic DFT calculations and experiments. Scale factors computed using the 3756-cm^{-1} experimental value for H_2O in the gas phase are 0.986 for PW91 (ADF) and 0.963 for B3LYP (NWChem). These scale factors predict the strong O−H stretching frequency for the $UO_2(OH)_2$ molecule at 3679 and 3703 cm^{-1}, which are both close to the 3670-cm^{-1} experimental value. However, note that the O−H stretching frequency is computed to be 16 cm^{-1} higher in the monohydroxide UO_2 species than in the dihydroxide species, the strong O═U═O stretching mode is calculated to be 50 cm^{-1} lower for the monohydroxide based on the NWChem calculations, and the O−H mode is calculated 6 cm^{-1} lower and the O═U═O mode 66 cm^{-1} lower based on ADF calculations. These predictions are in good agreement with our observations. Accordingly, the **b** bands are assigned to the OUO(OH) molecule.

The strong bands at 3670 and 920 cm^{-1} assigned here to the isolated $UO_2(OH)_2$ molecule in solid Ar may be compared to the strongest features at 3545 and 958 cm^{-1} in the IR spectrum of the solid compound.[4]

In the lower-frequency region, two absorptions at 569.0 and 546.8 cm^{-1} are associated with the $OUO(OH)_2$ molecule. The solid compound has a sharp absorption at 547 cm^{-1}. These absorptions are assigned to the strong modes calculated by NWChem at 572 and 556 cm^{-1}, and on the basis of computed isotopic shifts, these are mostly U−OH stretching and U−O−H bending modes, respectively. The $UO_2(OH)_2$ molecule identified here is highly interesting because it is likely involved in many chemical processes involving U or uranium oxide reactions with H_2O. We will discuss the electronic structure and bonding of this unique species in a separate section (see below).

$U(OH)_2$. The weak **d** absorption at 3740.7 cm^{-1} is observed with H_2O_2, and it increases upon annealing and decreases upon UV irradiation (Figure 1a−c). This band shifts to 2760.0 cm^{-1} with D_2O_2, which defines an appropriate H/D ratio, 1.3554, for an O−H stretching mode. This band is not observed with the H_2/O_2 reagent, but it shifted to 3729.3 cm^{-1} using ^{18}O-enriched H_2O (Table 2), which gives the $^{16}O/^{18}O$ ratio, 1.00306, for an O−H stretching mode. The 3740.7-cm^{-1} absorption is probably due to a $U(OH)_x$ species, and the two most likely x values are 2 and 4. Our ADF calculations predict the strongest $U(OH)_2$ bands at 3787 and 3786 cm^{-1}, which cannot be resolved in our spectra, and the strongest $U(OH)_4$ bands at 3787 and 3771 cm^{-1}, which should be observed as two equal-intensity bands. The H_2O experiment (Figure 5) shows the region 10−20 cm^{-1} lower than 3740 cm^{-1} to be free of absorption, which rules out the tetrahydroxide product species. Furthermore, our DFT calculations suggest that the simple uranium dihydroxide should fall 60−100 cm^{-1} higher than this mode for the $UO_2(OH)_2$ molecule. The single weak 3740.7-cm^{-1} band, which is observed 71 cm^{-1} higher, is therefore assigned to the straightforward U and H_2O_2 reaction product $U(OH)_2$. Note that both lower-energy isomers HU(O)OH and H_2UO_2 are observed here with more intense absorptions. The observation of 5-fold-more-intense 3740.7- and 2760.0-cm^{-1} bands in the H_2O experiments[14] argues for the dihydroxide assignment because the tetrahydroxide product would be much more complicated to form with the H_2O reagent, but the UO + H_2O reaction is straightforward, and this route was suggested for the HU(O)OH isomer. Note that the H_2O reaction gives about the same UO and UO_2 product band absorbances, but the H_2O_2 reaction favors substantially the UO_2 product.

The two lower-frequency bands at 570.5 and 527.3 cm^{-1} are assigned to the symmetric and antisymmetric U−OH stretching modes calculated in this region. On the basis of a mixed H/D isotopic triplet pattern, the 570.5-cm^{-1} X band was suggested to arise from a species containing a $U(OH)_2$ group,[14] which leads directly to the present assignment. We note that the deuterium counterpart bands at 551.8 and 514.3 cm^{-1} define shifts (18.7 and 13.0 cm^{-1}) that are in very good agreement with the calculated (17.3 and 14.4 cm^{-1}) shifts for this molecule. The yield of $U(OD)_2$ trapped in both D_2O_2

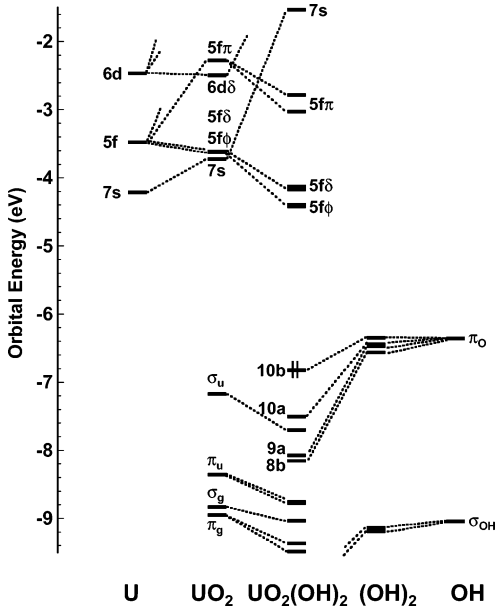

Figure 8. Correlation diagram of the scalar-relativistic energy levels of $UO_2(OH)_2$ and those of the constituent fragments U, UO_2, $(OH)_2$, and OH. The highest occupied molecular orbital of $UO_2(OH)_2$ is 10b and is illustrated by two electrons. The electron configurations of U, UO_2, and OH are $(7s)^1(5f)^3(6d)^1$, $(\pi_g)^4(\sigma_g)^2(\pi_u)^4(\sigma_u)^2(7s)^1(5f\phi)^1$, and $(\sigma_{OH})^2(\pi_O)^3$, respectively.

and D_2O experiments is higher than that found for the corresponding H species: apparently, the deuterated species rearranges more slowly to the more stable structural isomers than the hydrogenated counterpart. Accordingly, the species **d** bands are assigned to the uranium dihydroxide molecule $U(OH)_2$. This is the first experimental evidence for a pure uranium(II) hydroxide species, which would have interactions with Ar atoms in the first-coordination shell, as reported for $CUO(Ar)_x$ and $UO_2(Ar)_x$ complexes.[52,53]

Electronic Structure and Bonding of $UO_2(OH)_2$. As shown in Figure 7d, the $UO_2(OH)_2$ molecule adopts a structure with a near-linear uranyl unit and two bent OH groups. This structure suggests that the coordination of two OH groups has only moderately affected the UO_2 unit. From the PW91 calculations, the U═O distances are decreased from 1.813 Å in UO_2 to 1.805 Å in $UO_2(OH)_2$. At first glance, it seems nonintuitive that the U═O distances decrease upon binding of two OH groups. However, the decrease of the U═O distance is consistent with the oxidation state change from U^{IV} to U^{VI} and the electron removal from the U 7s orbital (see below). The correlation diagrams of the scalar-relativistic energy levels of U, UO_2, $UO_2(OH)_2$, and $(OH)_2$, OH calculated at the level of PW91/TZ2P using ADF code, are shown in Figure 8. As shown in previous calculations, when a U atom is bonded to two O atoms, four U-based electrons are transferred to the O atoms, leading to a U^{IV} $(7s)^1(5f\phi)^1$ ground-state electron configuration for UO_2.[46] Because of orbital interaction between U and O, the U 7s orbital is slightly increased in energy, whereas the U 5f and 6d orbitals are split into $5f\phi \sim 5f\delta \ll 5f\pi \ll 5f\sigma$ and $5d\delta \ll 6d\pi \ll 6d\sigma$, respectively, where the δ- and ϕ-type orbitals are almost nonbonding, while the σ- and π-type orbitals are pushed up in energy because of U═O bonding. Upon further binding of two OH groups to UO_2, two more U electrons are transferred to OH groups because the later has an $(\sigma_{OH})^2(\pi_O)^3$ electron configuration with low-energy unfilled valence orbitals. The energy of the U 7s orbital is significantly increased as a result of repulsive interaction with the OH lone pairs. The U $5f\phi$ and $5f\delta$ orbitals thus become the lowest unoccupied molecular orbitals (LUMOs), and the OH lone-pair 10b and 10a orbitals are the highest occupied frontier orbitals. The huge energy splitting between the 7s and $5f\phi/5f\delta$ orbitals upon OH coordination is similar to what we noted for the $UO_2(Ar)_5$ complex.[53] However, while the UO_2 complex with Ar atoms as ligands remains as a U^{IV} complex with a $(5f)^2$ configuration, the $UO_2(OH)_2$ complex is better viewed as a U^{VI} complex formed by UO_2^{2+} and OH^- ions because all of the U-based electrons are transferred to the ligands.

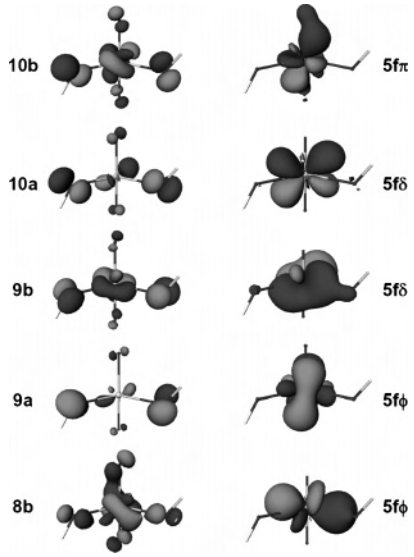

Figure 9. Three-dimensional contour surfaces (cutoff = 0.1 atomic unit) of the frontier molecular orbitals of $UO_2(OH)_2$. The highest occupied molecular orbital is 10b, and the LUMO is $5f\phi$. The orbital energy levels are shown in Figure 8.

Figure 9 shows the three-dimensional contour surfaces of some of the frontier orbitals of $UO_2(OH)_2$. It is clear that the bonding between UO_2 and OH groups can be considered as forming two weak U−OH bonds, leaving two lone pairs on each OH group. The U−OH bonds are dative, mainly involving U 6d and 5f orbitals to a lesser extent. Note that the U $5f\pi$ orbitals are degenerate in UO_2, but they are notably split in $UO_2(OH)_2$, indicating that U 5f orbitals indeed participate in the bonding. Similarly, the U 6d orbitals are not only significantly split in $UO_2(OH)_2$ but also pushed up in energy because the radially less contracted U 6d orbitals have a stronger orbital overlap with the OH orbitals than the 5f orbitals. The orbital interaction between U and OH also explains why structures with a bent U−OH unit are energetically favored and why $UO_2(OH)$ has a $(5f\phi)^1$ configuration rather than a $(7s)^1$ configuration.

(52) Li, J.; Bursten, B. E.; Liang, B.; Andrews, L. *Science* **2002**, *295*, 2242.
(53) Li, J.; Bursten, B. E.; Andrews, L.; Marsden, C. *J. Am. Chem. Soc.* **2004**, *126*, 3424.

Reaction Mechanisms. As we have found for group 2, 4, 11, 12, and 14 metals, the first step in the reaction with H_2O_2 is insertion to form the metal dihydroxide molecule.[17−22] The condensing matrix plays a crucial role in quenching of the large exothermicity of reaction (1a) and allowing the dihydroxide molecule to be relaxed and stabilized. In contrast, gas-phase group 2 metal atom reactions with H_2O_2 give the monohydroxide product.[54] The chemistry of the particular metal also comes into play during the relaxation process. The IV oxidation state HM(O)OH product is also formed with group 4 metals.[20] The VI oxidation state is particularly stable for U, and it is no surprise that rearrangement to the VI oxidation state H_2UO_2 species also occurs. Recall that H_2UO_2 was discovered in the U and H_2O reaction products[14] and that the IV and VI oxidation state products of reactions (1b) and (1c) are 24 and 36 kcal/mol, respectively, more stable than the II oxidation state product $U(OH)_2$ of reaction (1a) at the level of scalar-relativistic approximation. We note an order of magnitude higher yield of $U(OD)_2$ in these experiments than $U(OH)_2$, which suggests a kinetic isotopic effect on the rearrangements in reactions (1b) and (1c). Finally, there is a substantial yield of UO_2 in these experiments so H_2 elimination, reaction (1d), must also occur.

$$U + H_2O_2 \rightarrow [U(OH)_2]^* \rightarrow U(OH)_2 \quad (1a)$$

$$[U(OH)_2]^* \rightarrow HU(O)OH \quad (1b)$$

$$[U(OH)_2]^* \rightarrow H_2UO_2 \quad (1c)$$

$$[U(OH)_2]^* \rightarrow UO_2 + H_2 \quad (1d)$$

The second step is reaction of the products of reactions (1a)−(1d) with another H_2O_2 molecule [or the direct U reaction with a $(H_2O_2)_2$ dimer in the matrix cage] to form tetrahydroxide, as has been observed for groups 4 and 14 and Th.[20−22] In the relaxation of the energized uranium(IV) tetrahydroxide from highly exothermic reaction (2a), the stability of the U^{VI} state again comes into play with H_2 elimination to form the stable $UO_2(OH)_2$ molecule. The monohydroxide $UO_2(OH)$ is also produced. It appears that reactions (2b) and (2c) follow straightaway because we have no evidence for the relaxation and trapping of $U(OH)_4$.

$$U(OH)_2 + H_2O_2 \rightarrow [U(OH)_4]^* \quad (\Delta E = -184 \text{ kcal/mol}) \quad (2a)$$

$$[U(OH)_4]^* \rightarrow UO_2(OH)_2 + H_2 \quad (\Delta E = -2 \text{ kcal/mol}) \quad (2b)$$

$$[U(OH)_4]^* \rightarrow UO_2(OH) + OH + H_2 \quad (2c)$$

The major increase in the H_2O dimer and H_2O/HO radical complex bands upon UV irradiation in $U/H_2/O_2$ experiments provides mechanistic information. Apparently, reagent clusters give rise to OH radicals, which contribute to the yield of H_2O, the H_2O dimer, the H_2O/HO intermediate radical complex, and the uranium dioxide hydroxide products.

$$UO_2 + OH \rightarrow UO_2(OH) \quad (3a)$$

$$UO_2(OH) + OH \rightarrow UO_2(OH)_2 \quad (3b)$$

The reactions of U with $H_2 + O_2$ mixtures give UO_2 as the major product and smaller yields of $UO_2(OH)_2$, $UO_2(OH)$, and H_2UO_2. The group 2, 4, 11, and 12 dihydroxides were formed in the matrix reactions with $H_2 + O_2$ mixtures,[17−21] but the less-stable $U(OH)_2$ isomer was not trapped in the $U/H_2/O_2$ reaction system. However, $U(OH)_2$ was formed in much higher yield in the U/H_2O reaction system where UO was a major product, and the straightforward UO and H_2O insertion reaction (5) is proposed.

$$U + 2O_2 + H_2 \rightarrow UO_2 + O_2 + H_2 \rightarrow UO_2(OH)_2 \quad (4)$$

$$UO + HOH \rightarrow U(OH)_2 \quad (5)$$

Finally, it is interesting to compare these with the analogous reactions of Th with H_2O_2. We find $Th(OH)_4$ as the major product,[22] which is stable in the Th system where IV is the highest oxidation state. This lends credence to the role of $U(OH)_4$ as an intermediate in the formation of the U^{VI} product $UO_2(OH)_2$. The Th and U reaction systems both give $M(OH)_2$ and HM(O)OH as minor product species, but a substantially larger yield of UO_2 is observed as compared to ThO_2.

Conclusions

Reactions of laser-ablated U atoms and H_2O_2 molecules produce UO_2, H_2UO_2, $UO_2(OH)$, and $UO_2(OH)_2$ as major products and $U(OH)_2$ and HU(O)OH as minor products. Complementary information is obtained from similar reactions with D_2O_2 and with $H_2 + O_2$ mixtures and H_2O in excess Ar. Relativistic DFT calculations provide structures and frequencies in support of these assignments. First, the U atom reacting with H_2O_2 gives the $U(OH)_2$ insertion product, most of which rearranges to the more-stable HU(O)OH and H_2UO_2 isomers characterized in previous U/H_2O reactions.[14] The U atom reaction with two H_2O_2 forms energized $[U(OH)_4]^*$, which decomposes to the $UO_2(OH)_2$ molecule owing to the special stability of the U^{VI} oxidation state. In contrast, the major product in analogous Th reactions is the tetrahedral $Th(OH)_4$ molecule owing to the stable Th^{IV} oxidation state.

Acknowledgment. We gratefully acknowledge financial support for this research under NSF Grant CHE 03-52487 and helpful discussions with R. D. Hunt. This research was performed in part using the Molecular Science Computing Facility (MSCF) in the William R. Wiley Environmental Molecular Sciences Laboratory, a national scientific user facility sponsored by the U.S. Department of Energy's Office of Biological and Environmental Research and located at the Pacific Northwest National Laboratory. The Pacific Northwest National Laboratory is operated for the Department of Energy by Battelle.

IC052071A

(54) Li, M.; Coxon, J. A. *J. Chem. Phys.* **1995**, *102*, 2663; **1996**, *104*, 4961 and references cited therein.